

ON Semiconductor

Is Now

onsemi™

To learn more about onsemi™, please visit our website at
www.onsemi.com

onsemi and **onsemi** and other names, marks, and brands are registered and/or common law trademarks of Semiconductor Components Industries, LLC dba "**onsemi**" or its affiliates and/or subsidiaries in the United States and/or other countries. **onsemi** owns the rights to a number of patents, trademarks, copyrights, trade secrets, and other intellectual property. A listing of **onsemi** product/patent coverage may be accessed at www.onsemi.com/site/pdf/Patent-Marking.pdf. **onsemi** reserves the right to make changes at any time to any products or information herein, without notice. The information herein is provided "as-is" and **onsemi** makes no warranty, representation or guarantee regarding the accuracy of the information, product features, availability, functionality, or suitability of its products for any particular purpose, nor does **onsemi** assume any liability arising out of the application or use of any product or circuit, and specifically disclaims any and all liability, including without limitation special, consequential or incidental damages. Buyer is responsible for its products and applications using **onsemi** products, including compliance with all laws, regulations and safety requirements or standards, regardless of any support or applications information provided by **onsemi**. "Typical" parameters which may be provided in **onsemi** data sheets and/or specifications can and do vary in different applications and actual performance may vary over time. All operating parameters, including "Typicals" must be validated for each customer application by customer's technical experts. **onsemi** does not convey any license under any of its intellectual property rights nor the rights of others. **onsemi** products are not designed, intended, or authorized for use as a critical component in life support systems or any FDA Class 3 medical devices or medical devices with a same or similar classification in a foreign jurisdiction or any devices intended for implantation in the human body. Should Buyer purchase or use **onsemi** products for any such unintended or unauthorized application, Buyer shall indemnify and hold **onsemi** and its officers, employees, subsidiaries, affiliates, and distributors harmless against all claims, costs, damages, and expenses, and reasonable attorney fees arising out of, directly or indirectly, any claim of personal injury or death associated with such unintended or unauthorized use, even if such claim alleges that **onsemi** was negligent regarding the design or manufacture of the part. **onsemi** is an Equal Opportunity/Affirmative Action Employer. This literature is subject to all applicable copyright laws and is not for resale in any manner. Other names and brands may be claimed as the property of others.



A Simple DC SPICE Model for the LLC Converter

Prepared by: Christophe Basso
ON Semiconductor

ON Semiconductor®

<http://onsemi.com>

APPLICATION NOTE

The resonant LLC topology, member of the Series Resonant Converters (SRC), begins to be widely used in consumer applications such as LCD TVs or plasma display panels. In these particular applications, the output power level ranges from 100 W up to 600 W. Designing an LLC converter requires to know the evolution of its DC transfer function in order to properly select the various elements the resonant circuit is made of. This application note shows us how a simple SPICE model operated in DC sweep, can help us in designing an LLC converter using the NCP1395 controller.

The LLC Topology

Figure 1 shows the structure of this resonant converter. A 50% duty cycle half-bridge delivers high voltage square waves swinging from 0 to the input voltage V_{in} to a resonating circuit. By adjusting the frequency via a voltage-controlled oscillator (VCO), the feedback loop can adjust the output level depending on the power demand.

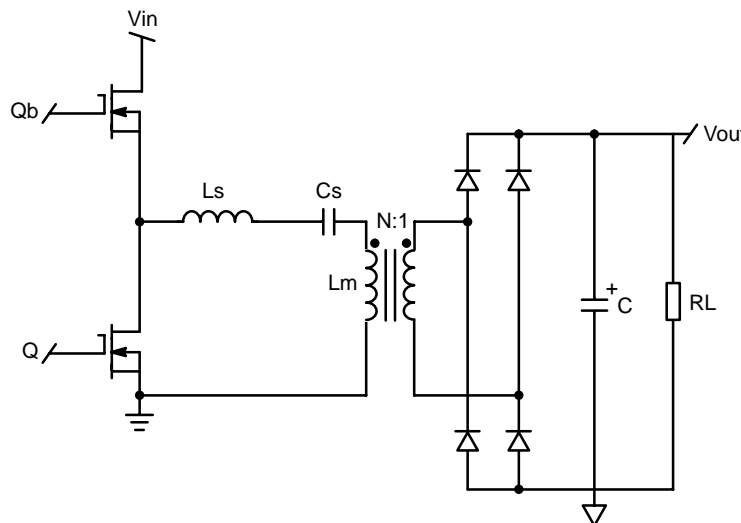


Figure 1. The LLC Topology Uses a Half-Bridge to Drive the Resonant Circuit

The resonating circuit is made of a capacitor, C_s , in series with two inductors, L_s and L_m . One of these inductors, L_m , represents the magnetizing inductor of the transformer and creates one resonating point together with L_s and C_s . We can quickly see that the reflection of the load over this inductor will either make it disappear from the circuit (L_m is fully short-circuited by a reflected R_L of low value at heavy load currents) or will make it stay in series with the series

inductor L_s in light load conditions. As a result, depending on the loading conditions, the resonant frequency will move between a minimum and a maximum:

$$F_{\max} = F_s = \frac{1}{2\pi\sqrt{L_s C_s}} \quad (\text{eq. 1})$$

$$F_{\min} = \frac{1}{2\pi\sqrt{(L_s + L_m)C_s}} \quad (\text{eq. 2})$$

The frequency of operation depends on the power demand. For a low power demand, the operating frequency is rather high, away from the resonating point. To the contrary, at high power, the control loop reduces the switching frequency and approaches one of the resonant frequency to deliver the necessary amount of current to the load. The principle of the LLC operation assumes that the circuit operates close to its resonant frequency. Hence, sinusoidal variables are in play. Therefore, as the vast majority of harmonics are removed, we can imagine the

circuit as a bandpass filter for the square wave excitation. This technique is called First Harmonic Approximation (FHA) and consists of replacing the square wave input (the half-bridge signal) by its fundamental value. The peak fundamental of a 50% duty cycle square wave signal toggling between 0 and V_{in} is:

$$V_{fund, peak} = \frac{2}{\pi} V_{in} \quad (eq. 3)$$

Hence, the equivalent circuit of Figure 2:

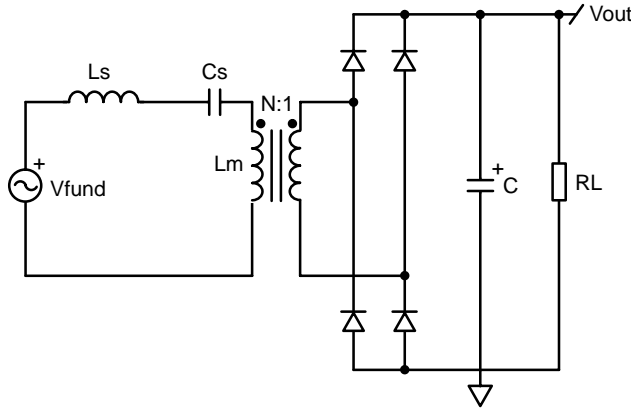


Figure 2. Using FHA, we can draw an equivalent “sinusoidal” schematic of our LLC converter.

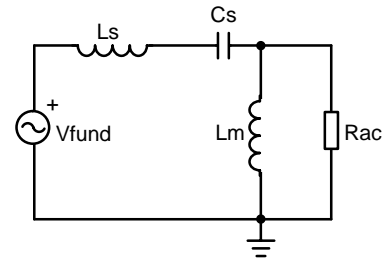


Figure 3. An equivalent load is reflected on the primary inductance L_m .

If we want to study our resonant network using FHA, we must get rid of the diode bridge and find a way to place an equivalent resistor “seen” from the left side of the bridge. Figure 3 is the circuit we actually would like to have. If we closely look at Figure 2, we can see a current-fed structure, otherwise stated, into a network made of the transformer and

the load. This can be further demonstrated by the direct connection of the capacitor across the bridge output, without a smoothing inductor as it is the case with Series Parallel Resonant converter. This observation will help deriving the equivalent resistor R_{ac} , as indicated by Figure 4 where we purposely removed the transformer for the sake of simplicity:

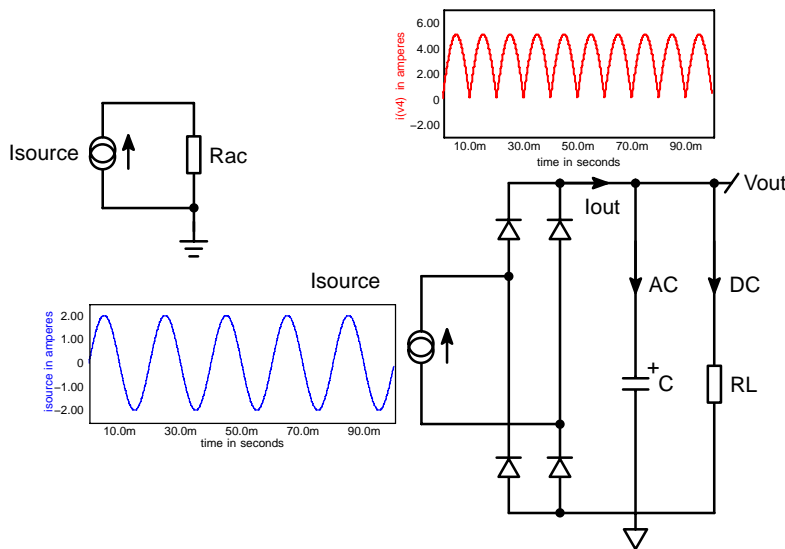


Figure 4. A simplified representation helps us to derive R_{ac} in a few lines of algebra.

The upper left corner of Figure 4 represents the AC source delivering current to the equivalent load resistor we are looking for, R_{ac} . The power delivered by this source is simply the rms current squared multiplied by the resistor:

$$P_{in} = I_{source, rms}^2 R_{ac} = \left(\frac{I_{source, peak}}{\sqrt{2}} \right)^2 R_{ac} = \frac{I_{source, peak}^2}{2} R_{ac} \quad (eq. 4)$$

The output power can be quickly expressed since the current that flows in R_L is the average current of I_{out} (all the AC current flows into C). Hence:

$$P_{out} = (I_{out, avg})^2 R_L = \left(\frac{2I_{source, peak}}{\pi} \right)^2 R_L = \frac{4R_L}{\pi^2} I_{source, peak}^2 \quad (eq. 5)$$

Assuming we have a 100% efficiency, then the input power equals the output power:

$$\frac{I_{source, peak}^2}{2} R_{ac} = \frac{4R_L}{\pi^2} I_{source, peak}^2 \quad (eq. 6)$$

Extracting R_{ac} leads to:

$$R_{ac} = \frac{8R_L}{\pi^2} \quad (eq. 7)$$

If we now include the transformer as on Figure 1, the final reflected load becomes:

$$R_{ac} = \frac{8R_L N^2}{\pi^2} \quad (eq. 8)$$

Figure 3 shows the equivalent FHA schematic. What we want is to refine this model with all equivalent components: we must find a relationship between the DC output voltage actually applied across R_L and the DC input voltage V_{in} . Figure 5 displays the idea behind this reasoning, again with the transformer removed for simplicity:

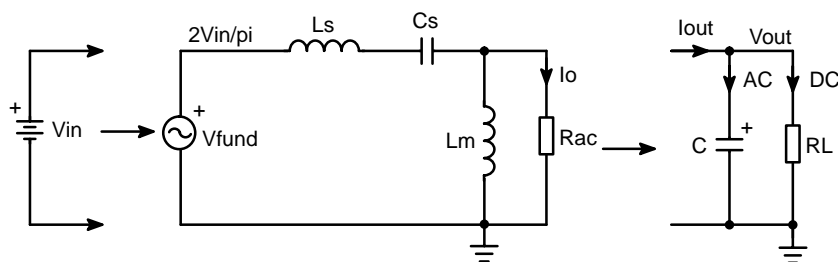


Figure 5. We want to find the relationship between the output of our equivalent network and the real DC output voltage.

The current flowing into R_{ac} is the following:

$$I_{o, peak} = \frac{V_{o, peak}}{R_{ac}} \quad (eq. 9)$$

Replacing R_{ac} by its definition (Equation 7):

$$I_{o, peak} = \frac{V_{o, peak} \pi^2}{8R_L} \quad (eq. 10)$$

The DC voltage applied to the load is nothing else than the DC component (the averaged value) of the rectified half-wave $I_{o, peak}$. Thus:

$$I_{out} = \frac{V_{o, peak} \pi^2}{8R_L} \cdot \frac{2}{\pi} = \frac{V_{o, peak} \pi}{4R_L} \quad (eq. 11)$$

Now, the output voltage is simply Equation 11 multiplied by R_L :

$$V_{out} = \frac{V_{o, peak} \pi}{4R_L} R_L = \frac{V_{o, peak} \pi}{4} \quad (eq. 12)$$

Therefore, the output voltage obtained across R_{ac} has the following value, now including the transformer:

$$V_{o, peak} = \frac{V_{out} 4N}{\pi} \quad (eq. 13)$$

The final equivalent model looks like the following:

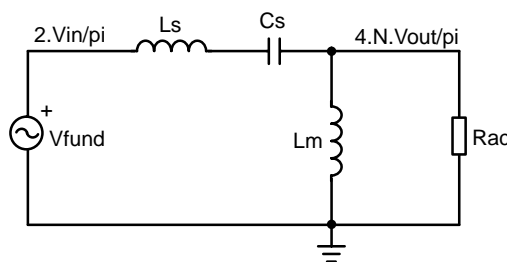


Figure 6. The Final FHA Model of our LLC Converter

We can see now that if we compute the transfer ratio between V_{out} and V_{in} , several factors will need to appear in order to get the right levels. Let us start with the transfer ratio of Figure 6 that can be obtained via the following lines:

$$\frac{4N V_{out}}{\frac{\pi}{2V_{in}}} = M \quad (eq. 14)$$

Rearranging Equation 14:

$$\frac{V_{out}}{V_{in}} = \frac{1}{2N} M \quad (\text{eq. 15})$$

$$M = \left| \frac{sL_m \parallel R_{ac}}{sL_m \parallel R_{ac} + sL_s + \frac{1}{sC_s}} \right| \quad (\text{eq. 16})$$

Now, it is time to calculate M ...

The brute force result of this module calculation is the following ugly result:

$$M = \sqrt{\frac{1}{\frac{\omega^2 L_s^2}{R_{ac}^2} + 1 - \frac{2Z_0^2}{R_{ac}^2} + \frac{2}{ratio} + \frac{1}{ratio^2} + \frac{1}{R_{ac}^2 C_s^2 \omega^2} - \frac{2}{L_p C_s \omega^2} - \frac{2Z_0^2}{L_p^2 \omega^2} + \frac{1}{L_p^2 C_s^2 \omega^4}}} \quad (\text{eq. 17})$$

Where: $Z_0 = \sqrt{\frac{L_s}{C_s}}$ $ratio = \sqrt{\frac{L_m}{L_s}}$ $R_{ac} = \frac{8R_L N^2}{\pi^2}$ $Q = \frac{N^2 R_L}{Z_0}$

Please note that in no-load conditions ($R_{ac} = \infty$) Equation 17 simplifies to a simple impedance divider:

$$M = \frac{L_m}{L_m + L_s} \quad (\text{eq. 18})$$

This represents a design factor when selecting the magnetizing inductance and the series inductance if no-load condition can occur. Hence, once the turn-ratio and these elements has been selected, you can immediately see if the converter will accept no-load conditions, whatever the VCO excursion is. Fortunately, the NCP1395 authorizes skip cycle and will naturally prevent loss of regulation in this particular case by interrupting the switching frequency as the feedback loop reaches a user-selectable level.

Assembling Sources for the DC Model

We almost now have everything needed to start assembling our Analog Behavioral Modeling sources (ABM) to build the model. Figure 7 represents the frame of the model where R_{ac} receives a current proportional to M and the input voltage:

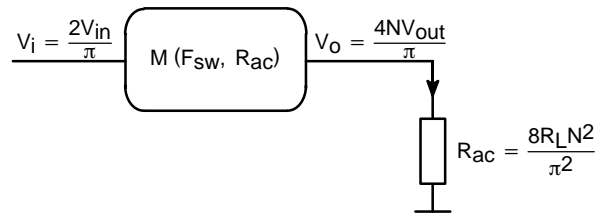


Figure 7. The output voltage generates a voltage across R_{ac} . But this voltage is not V_{out} ...

How do we link the current I crossing R_{ac} to our real output current flowing through the load? Let us express it using Ohm's law:

$$I = \frac{V_o}{R_{ac}} = \frac{4N V_{out}}{\pi} \frac{\pi^2 N^2}{8R_L} = \frac{2M V_i}{R_{ac} \pi} \quad (\text{eq. 19})$$

Replacing V_i by Equation 3, we have an updated current definition:

$$I = \frac{2M}{R_{ac} \pi} \frac{2V_{in}}{\pi} = \frac{4M V_{in}}{R_{ac} \pi^2} \quad (\text{eq. 20})$$

We can also replace R_{ac} thus:

$$I = \frac{4M V_{in}}{\pi^2} \frac{\pi^2}{8N^2 R_L} = \frac{M V_{in}}{2N^2 R_L} \quad (\text{eq. 21})$$

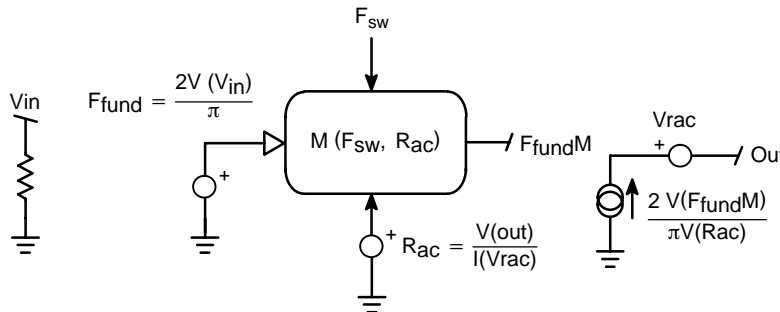


Figure 8. The model looks for the current circulating inside R_{ac} and forces a proportional current on the output node.

Further to a few experiments on SPICE, we found that Equation 19 gave better results than Equation 21 in terms of initial bias point calculation. We thus adopted it for the model whose final theoretical architecture appears on Figure 8. We can recognize sources performing the previously derived equations like the fundamental amplitude calculation or the output current generator. The node “out” can directly connect to the load via a transformer and the R_{ac} value gets calculated via a separated source. Its result directly enters the M generator to further drive the final current source. Figure 9 portrays the real SPICE arrangement using INTUSOFT’s *IsSpice*. Some precautions are taken to avoid division by zero during the bias point calculations. This is “+1u” add on to some terms. Here are the various sources functions:

- B5: The error voltage is expressed in V and further converted to kHz via B5: $1.0 \text{ V} = 100 \text{ kHz}$
- B6: It calculates the fundamental based on a half-bridge configuration and the input node *vin*
- B1: Elaborates ω from B5
- B7: This source calculates R_{ac} according to Equation 7
- B3: It is the M parameter as Equation 17 describes it
- B2: Calculates the input current drawn from the source based on the total converter efficiency ETA
- B4: The final current source delivering Equation 19 current level
- A few parameters need to be passed to get all the necessary coefficients the above equations require

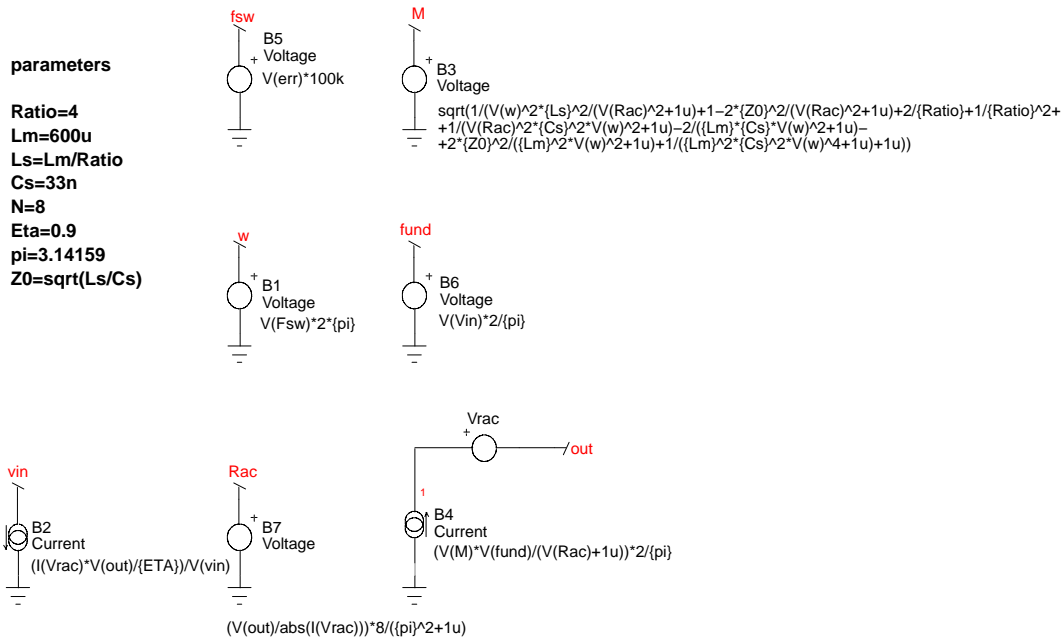


Figure 9. The Final Model in INTUSOFT’s *IsSpice*

Based on this configuration, we have encapsulated the model under a simple symbol and placed in an application circuit. This is what appears on Figure 10. In this circuit, a DC source is connected to the error input and generates the control frequency. Here, 572 mV corresponds to 57.2 kHz.

The parameters column, on the left side, includes the selected elements for this 24 V/250 W converter operated from a 380 V input voltage. The various sources are placed there to display some operating parameters we will need for the final curve display.

AND8255/D

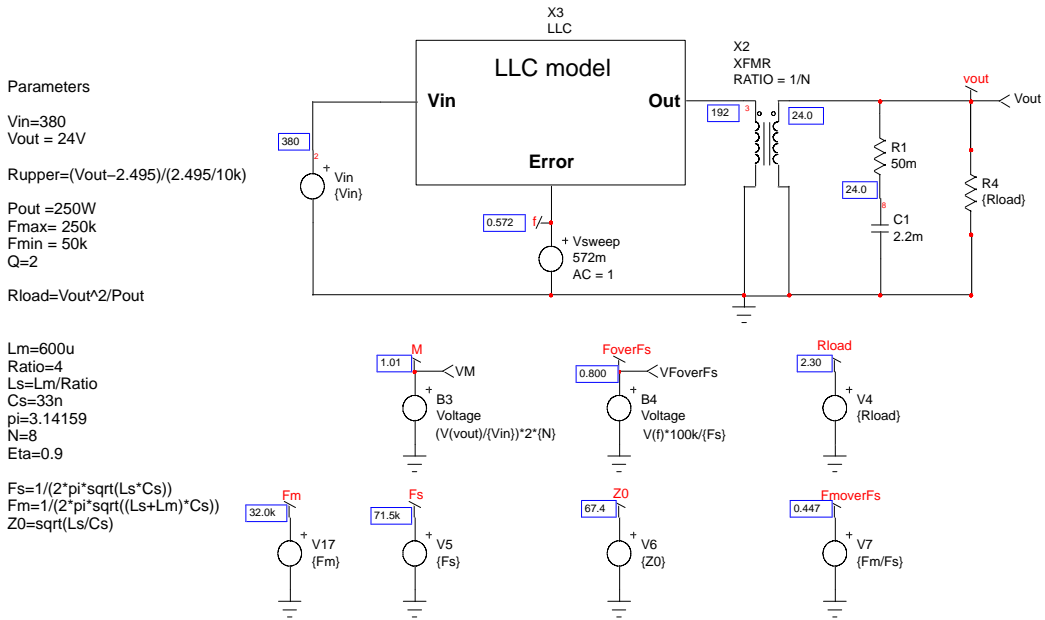


Figure 10. The model once encapsulated is ready for the DC sweep.

If we now sweep the source V_{sweep} from 100 mV (10 kHz) to 2.0 V (200 kHz) and monitor M (the ratio as defined by Equation 15) we can check for the model validity to predict voltage conversion ratios. We can then adjust the ratio

between the magnetizing inductance L_m and the series inductance L_s and see how M is affected while the quality coefficient Q is varied ($Q = \frac{N^2 R_L}{Z_0}$):

- 1 vm 2 vm#a6 3 vm#a7 4 vm#a8 5 vm#a9

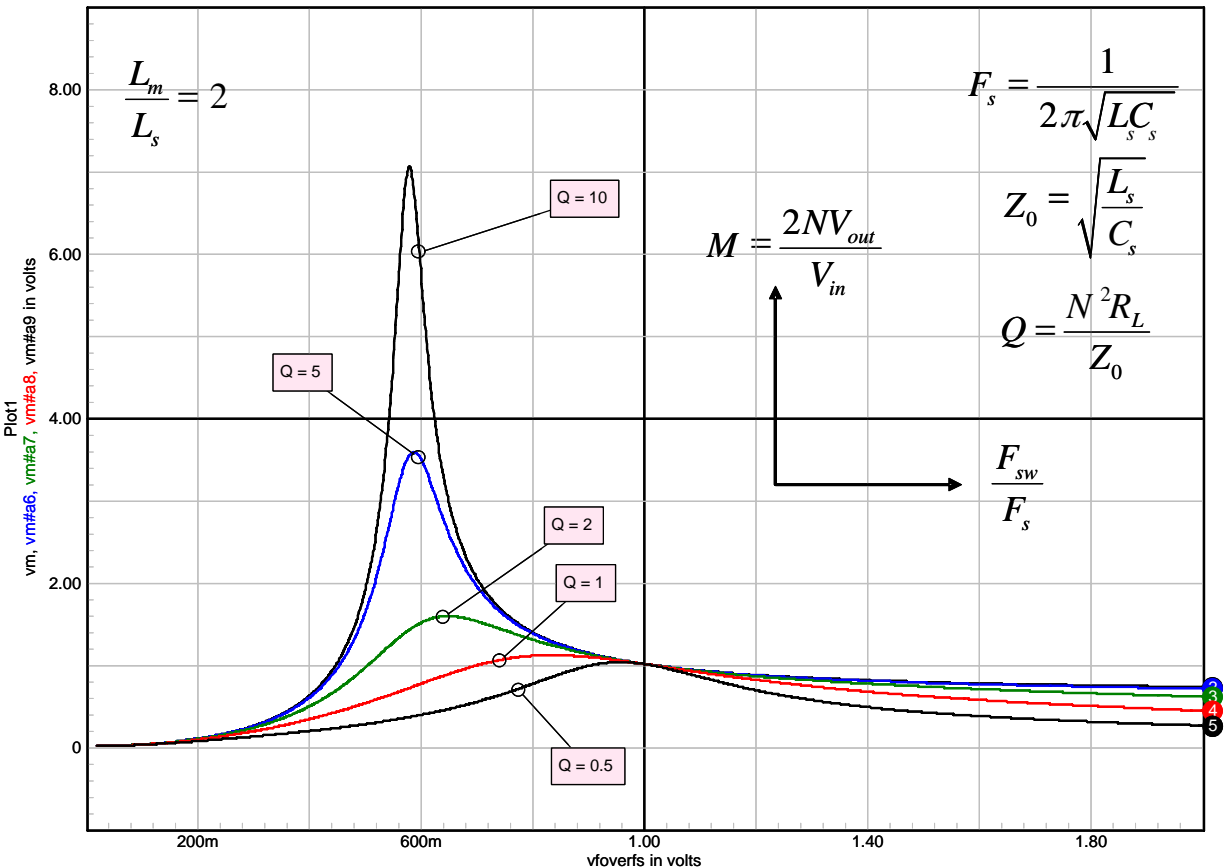


Figure 11. The transfer function for a ratio between L_m and L_s of 2.

AND8255/D

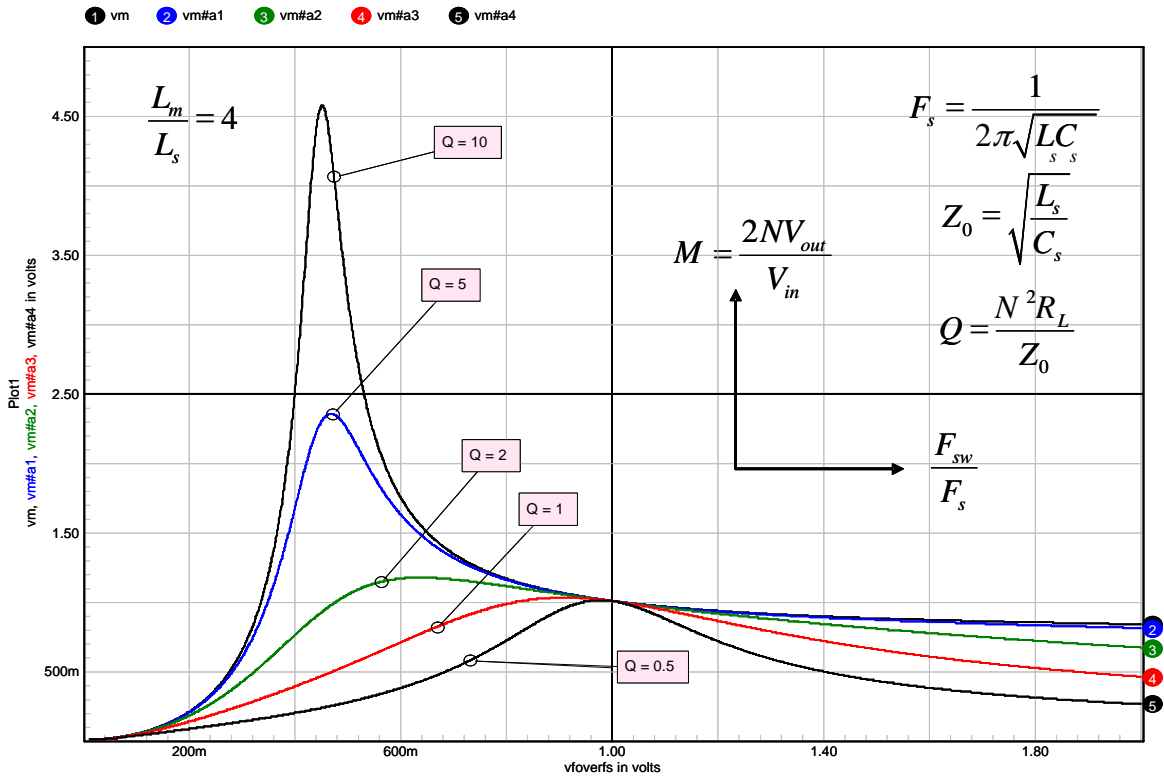


Figure 12. Same as above, but the ratio is 4.

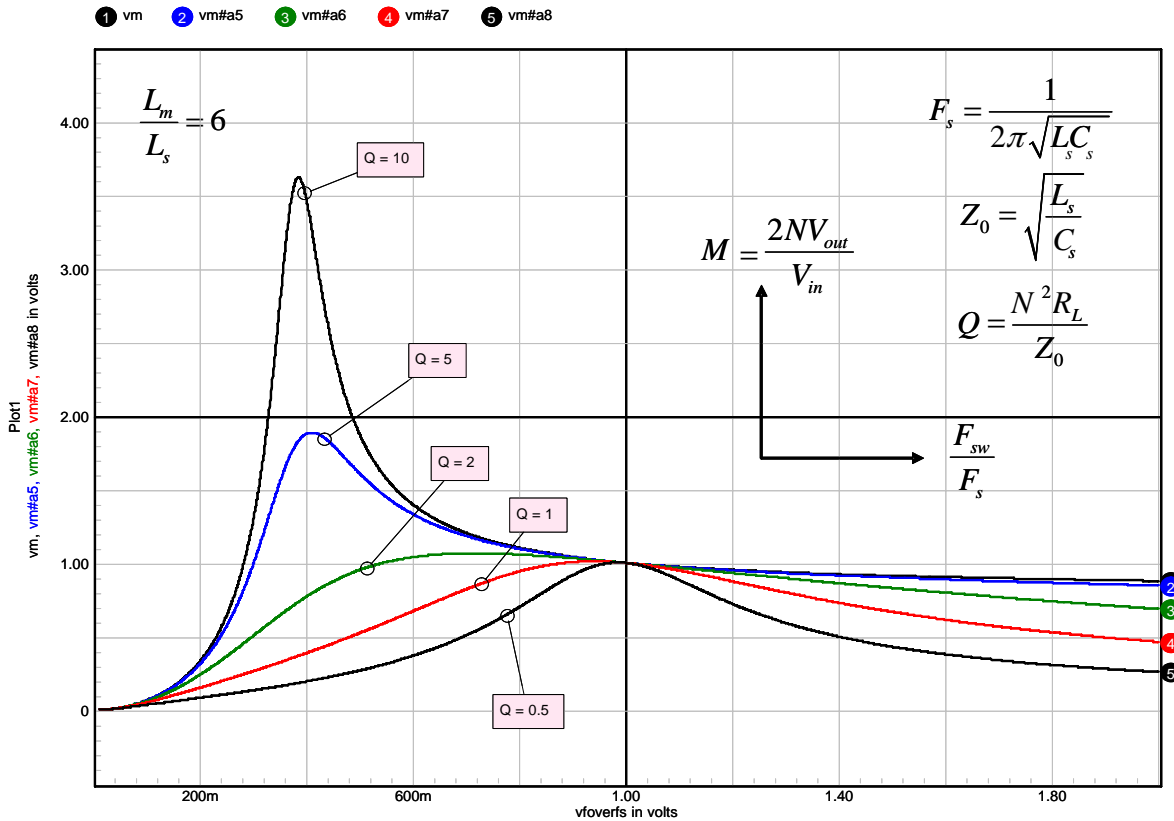


Figure 13. Same as above, but the ratio is 6.

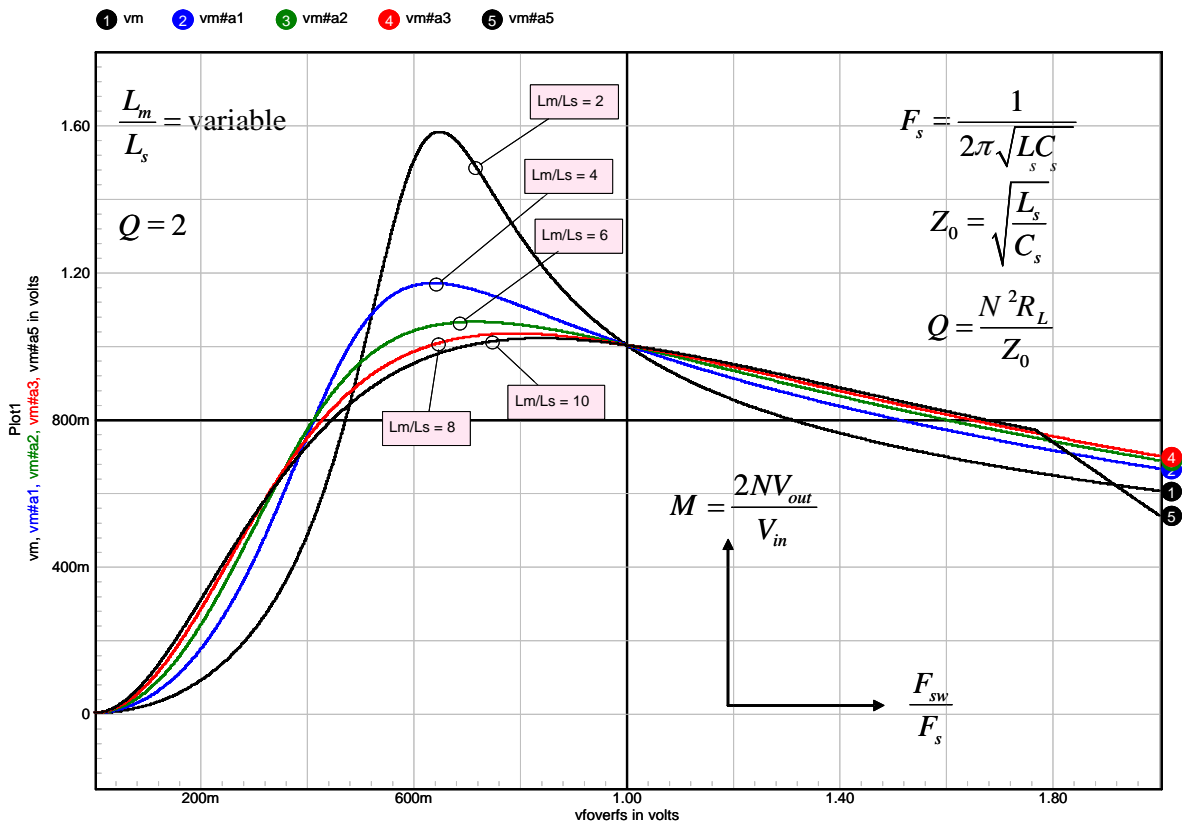


Figure 14. Conversion ratio for a given quality coefficient ($Q = 2$) but the ratio is varied from 2 to 10.

From the above curves, a few comments can be made:

1. As the ratio between the magnetizing inductance L_m and the series inductance L_s increases, the transfer ratio between V_{in} and V_{out} goes down (max $M = 7$ on Figure 11, ratio = 2 and max $M = 3.5$ on Figure 13, for a ratio of 6).
 2. The separation between F_{max} and F_{min} (Equations 1 and 2) widens and thus requires a larger regulation–frequency range:
- Figure 11: for $Q = 5$, we obtain a ΔM of 1 for a Δf of 0.065
 - Figure 13: for $Q = 5$, we obtain a ΔM of 1 for a Δf of 1.2
3. From Figure 14, as the ratio increases, the DC gain flattens and regulating in light load conditions becomes difficult (weak variation of M versus f_{sw}).

The Internal Modulator

The NCP1395 features a Voltage–Controlled Oscillator (VCO) switching from 50 kHz up to 1.0 MHz. You drive its pin number 5 to increase or decrease the frequency. However, for security reasons, there is a threshold above which the sweep actually starts. Below this threshold (1.3 V typical), the frequency does not change and stays at the minimum value imposed by the resistor on pin 1. The

modulator section we are going to describe thus accounts for this threshold but also for the upper limit above which the variation slope is null (6.0 V). By changing minimum and maximum frequency limits, the small signal slope of the VCO is also changed what the modulator also reflects. Figure 15 shows the internal section of this box:

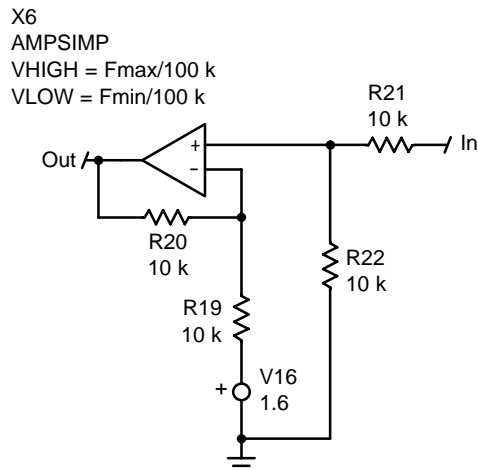


Figure 15. The modulator introduces a threshold and tailors the minimum and maximum switching frequency excursions.

AND8255/D

Once wired together, the final test circuit looks like that of Figure 16:

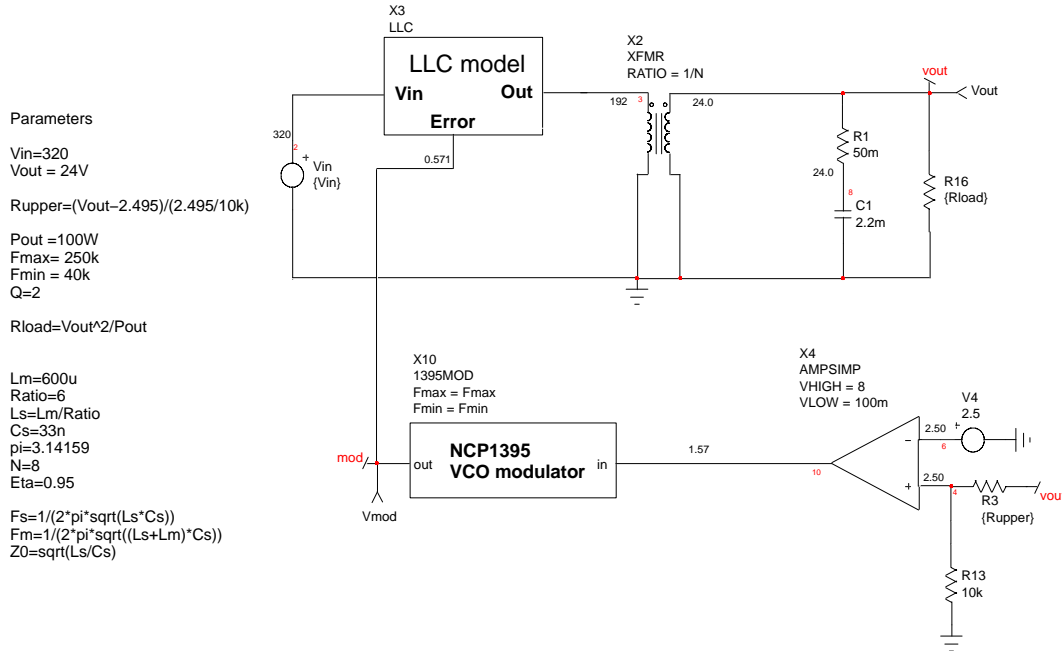


Figure 16. The complete test circuit including the LLC DC model and its VCO modulator.

Running a DC point analysis gives the operating frequency for given input and output conditions. The output capacitor has been kept in place, but does not play any role in DC. The right side OPAMP just helps to close the loop in DC and have the right operating point automatically setup, e.g. 24 V at a given output power level. In this example, the system delivers 100 W and operates at a switching frequency of 57 kHz. The voltage on the NCP1395 pin reaches 1.6 V to deliver these 57 kHz.

Unfortunately, it is not possible to use this model as a small-signal tool to reveal the Bode plot of an LLC converter. This is because the LLC converter operates in various regions, depending on its switching frequency and the distance of this switching frequency to the resonating frequency imposed by L_s and C_s . As such, the LLC converter behaves as different order systems depending on the region where it operates:

- For switching frequencies away from the resonant frequency F_{max} (set by L_s and C_s , Equation 1), the low-frequency small-signal response shows a first order behavior with a single pole given by the load and the output capacitor:

$$f_p = \frac{1}{2\pi R_{load} C_{out}} \quad (\text{eq. 22})$$

In this operating mode, a high-frequency double pole exists, but its location does not significantly affect the low frequency portion of the Bode plot. This double pole is located at the beat frequency between the switching F_{sw} and F_{max} , the series resonant frequency.

- When the distance between F_{sw} and F_{max} reduces, that is to say the feedback loop answers to an increased power demand, root-locus analysis shows that the double pole splits: one pole moves toward the high frequency region whereas the other one goes down the low frequency area until it joins the pole given by Equation 22: the LLC converter now shows a second order behavior.

Design Example Using the Model

Let us see how we can use the DC model to select the right components for a design example. The specifications could look like the following:

- $V_{in,max} = 400$ Vdc
- $V_{in,min} = 350$ Vdc
- $V_{out} = 24$ V
- $I_{out,max} = 10$ A
- $I_{out,min} = \text{No load}$
- $F_{sw,min} = 70$ kHz

Since we can easily implement skip cycle in the NCP1395, the no-load condition does not represent a significant problem at the design phase. For this particular design, we will arbitrarily adopt a ratio of 6 between L_m and L_s and an operating quality factor Q of 1. Another application note will detail how these choices affect the LLC operation and in particular, component stress. To help select the resonant devices, we can use Figure 17 graphic representation of M :

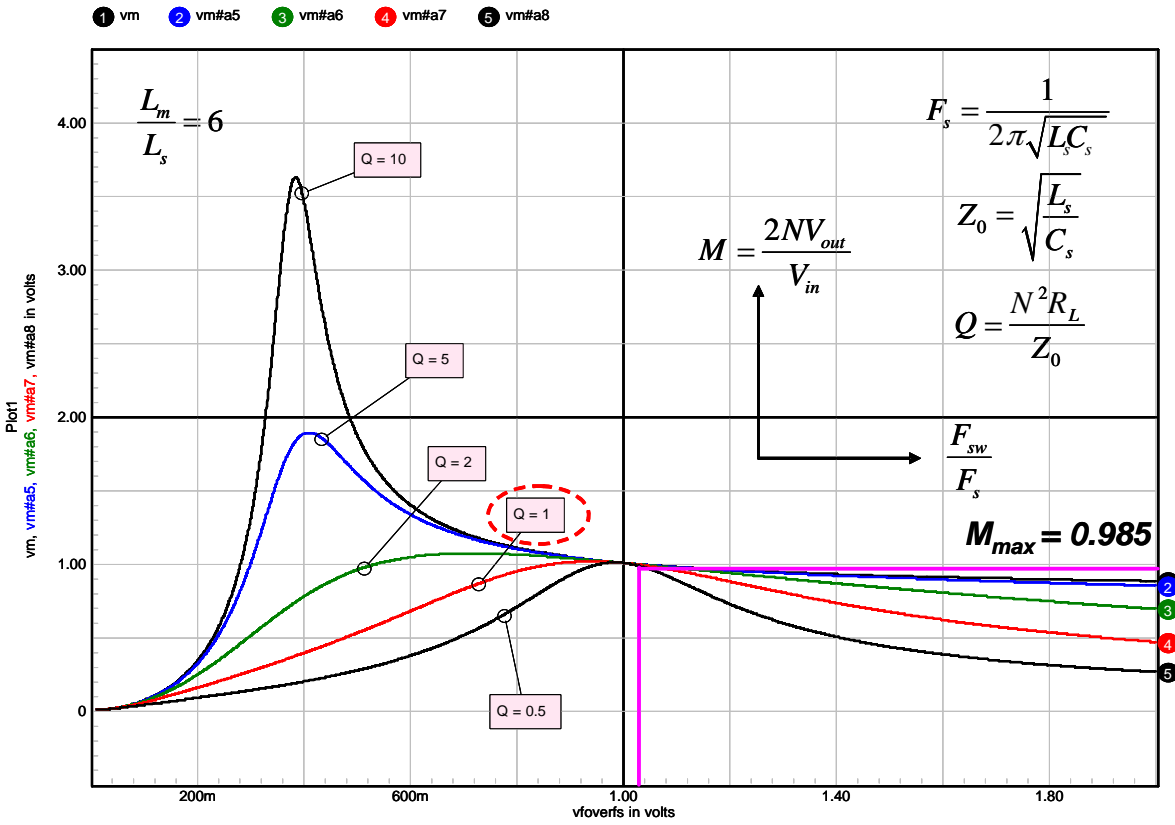


Figure 17. This picture shows the different transfer ratio depending on the loading and the operating frequency.

From this plot, after locating the curve displaying $Q = 1$, we go on its right side to operate on ZVS at full load. We can see a maximum M value of 0.985 and a ratio between the resonant frequency F_s and the switching frequency F_{sw} of 1.035. Hence we can immediately calculate our component values following the steps:

1. Turn ratio from Equation 15: $\frac{V_{out}}{V_{in}} = \frac{M}{2N}$ then
$$N = \frac{MV_{in, min}}{2V_{out}} = \frac{0.985 \times 350}{2 \times 24} = 7.2 \quad (\text{eq. 23})$$
 Transformer featuring a turn-ratio of $N_p:N_s = 7:1$.
2. From Figure 17 abscisse, the relationship between the resonant frequency and the switching frequency is 1.035. Hence, the resonant frequency will be set to:
$$F_s = \frac{F_{sw, min}}{1.035} = \frac{70k}{1.035} = 67.6 \text{ kHz} \quad (\text{eq. 24})$$
3. We have purposely selected an operating Q of 1. Knowing the relationship between Q and the characteristic impedance of the resonating network, we can obtain L_s definition:

$$Z_0 = \sqrt{\frac{L_s}{C_s}} \text{ or } C_s = \frac{L_s}{Z_0^2} \quad (\text{eq. 25})$$

In Equation 1, we can insert Equation 25:

$$F_s = \frac{1}{2\pi\sqrt{L_s C_s}} = \frac{1}{2\pi\sqrt{L_s \frac{L_s}{Z_0^2}}} \quad (\text{eq. 26})$$

Rearranging Equation 26 leads to:

$$L_s = \frac{Z_0}{2\pi F_s} \quad (\text{eq. 27})$$

From our previous definitions, we know:

$$Q = \frac{N^2 R_L}{Z_0} \quad (\text{eq. 28})$$

$$\text{hence } Z_0 = \frac{N^2 R_L}{Q} = \frac{7.22 \times 2.3}{1} = 120$$

Therefore, according to Equation 27, the final L_s calculation becomes:

$$L_s = \frac{120}{2 \times \pi \times 67.6 \text{ k}} = 282 \mu\text{H} \quad (\text{eq. 29})$$

4. Due to the selected ratio of 6, we obtain L_m :

$$L_m = L_s \text{Ratio} = 1.7 \text{ mH} \quad (\text{eq. 30})$$

5. The resonant capacitor value is straightforward due to Equation 26:

$$C_s = \frac{1}{4\pi^2 F_s^2 L_s} = \frac{1}{39.5 \times 4.569 \text{ Meg} \times 282\mu} = 20 \text{ nF} \quad (\text{eq. 31})$$

6. The RMS current circulating in the inductor but also the capacitor is [1]:

$$I_{Ls, rms} = \frac{\sqrt{2} \pi \cdot I_{out, max}}{4N}$$

$$\sqrt{1 + \left(\frac{4N^2 V_{out}}{\pi^3 F_{sw, min} L_m I_{out, max}} \right)^2} = 1.7 \text{ A} \quad (\text{eq. 32})$$

7. The peak voltage across the resonating capacitor will be:

$$V_{Cs, peak} = \frac{V_{in, max}}{2} + \frac{\sqrt{2} I_{Ls, rms}}{2\pi F_{sw, min} C_s} = 488 \text{ V} \quad (\text{eq. 33})$$

A 3.0 A/600 V capacitor will then be selected.

8. Based on the selected value, we can check the no-load conditions and see what value M will take, using Equations 15 and 18:

$$V_{out, noload} = \frac{L_m V_{in, max}}{(L_m + L_s) 2N} = 23.8 \text{ V} \quad (\text{eq. 34})$$

Hence, no load regulation could theoretically be ensured without entering skip-cycle.

Calculated values can now be entered in the LLC model and the output voltage observed, versus the swept frequency. Figure 18 shows output results at two different input voltages:

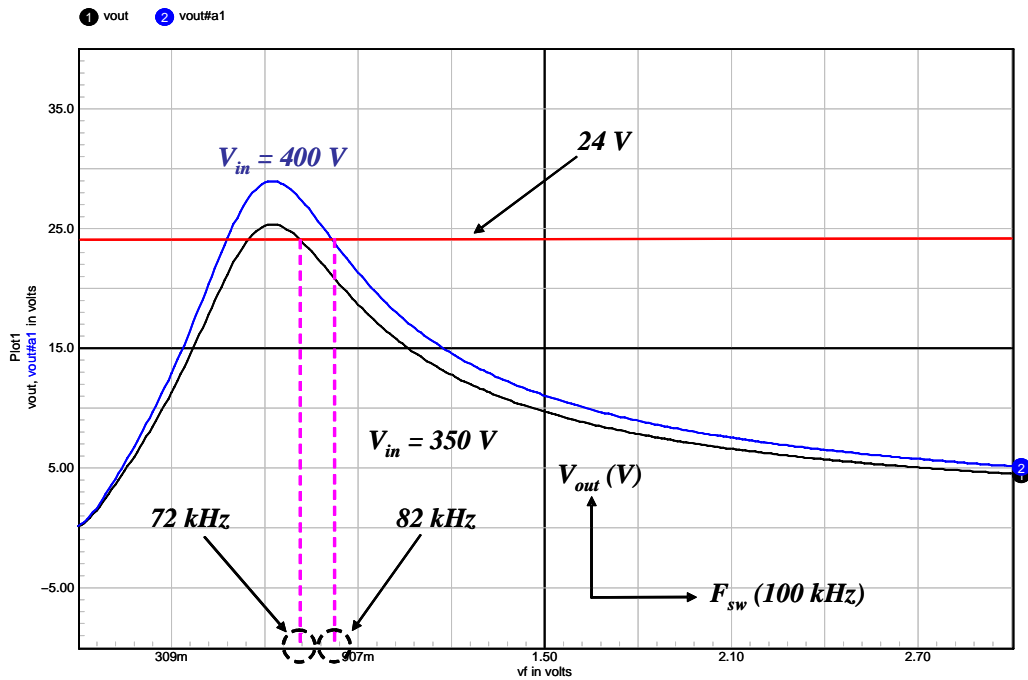


Figure 18. Frequency Variations Full Load at Different Input Voltages

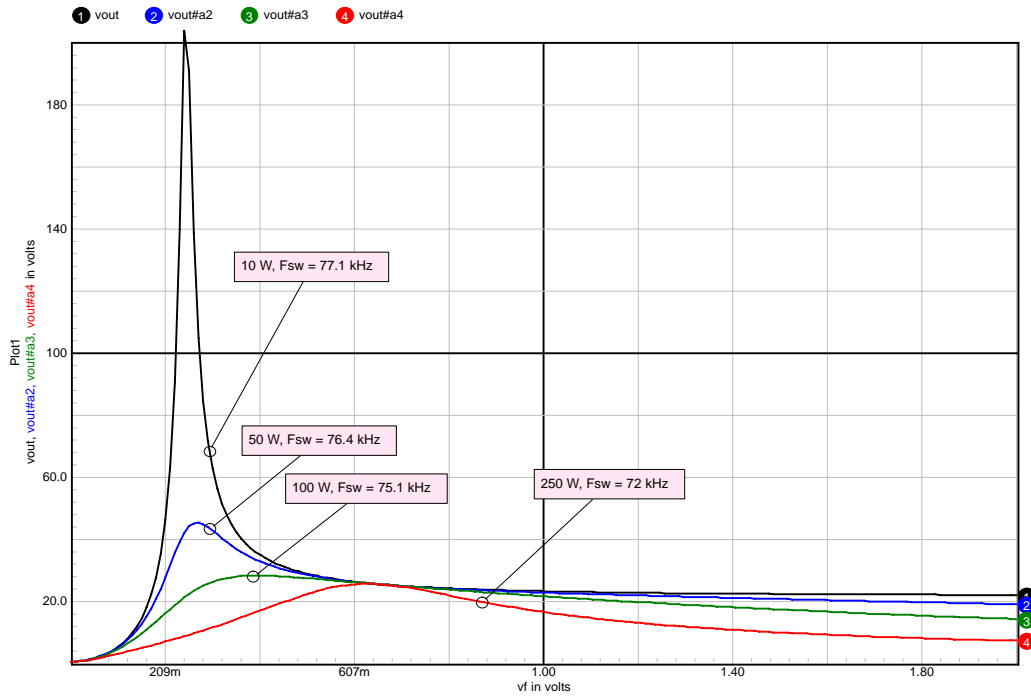


Figure 19. Frequency Evaluation for Variable Load Conditions, Input Voltage is 350 Vdc

Figure 19 plots the evolution of the switching frequency versus different load conditions. Design choices imply a frequency variation of 5.0 kHz between light load and full load. Different choices of L_m and L_s would have given wider or narrower variations.

Conclusion

This paper details how a simplified DC model for the LLC converter was derived. Based on first harmonic approximation, the precision of the approach fades away as

the operating frequency deviates from the resonant frequency. Nevertheless, the model can be useful for a quick test of calculated components and see whether the operating frequency and output voltage are within the range of interest.

References

1. M. Jovanovic, “Principle of Resonant Power Conversion”, in-house seminar, Toulouse 2004.
2. NCP1395 data sheet, www.onsemi.com.

ON Semiconductor and are registered trademarks of Semiconductor Components Industries, LLC (SCILLC). SCILLC reserves the right to make changes without further notice to any products herein. SCILLC makes no warranty, representation or guarantee regarding the suitability of its products for any particular purpose, nor does SCILLC assume any liability arising out of the application or use of any product or circuit, and specifically disclaims any and all liability, including without limitation special, consequential or incidental damages. “Typical” parameters which may be provided in SCILLC data sheets and/or specifications can and do vary in different applications and actual performance may vary over time. All operating parameters, including “Typicals” must be validated for each customer application by customer’s technical experts. SCILLC does not convey any license under its patent rights nor the rights of others. SCILLC products are not designed, intended, or authorized for use as components in systems intended for surgical implant into the body, or other applications intended to support or sustain life, or for any other application in which the failure of the SCILLC product could create a situation where personal injury or death may occur. Should Buyer purchase or use SCILLC products for any such unintended or unauthorized application, Buyer shall indemnify and hold SCILLC and its officers, employees, subsidiaries, affiliates, and distributors harmless against all claims, costs, damages, and expenses, and reasonable attorney fees arising out of, directly or indirectly, any claim of personal injury or death associated with such unintended or unauthorized use, even if such claim alleges that SCILLC was negligent regarding the design or manufacture of the part. SCILLC is an Equal Opportunity/Affirmative Action Employer. This literature is subject to all applicable copyright laws and is not for resale in any manner.

PUBLICATION ORDERING INFORMATION

LITERATURE FULFILLMENT:
 Literature Distribution Center for ON Semiconductor
 P.O. Box 5163, Denver, Colorado 80217 USA
Phone: 303-675-2175 or 800-344-3860 Toll Free USA/Canada
Fax: 303-675-2176 or 800-344-3867 Toll Free USA/Canada
Email: orderlit@onsemi.com

N. American Technical Support: 800-282-9855 Toll Free USA/Canada
Europe, Middle East and Africa Technical Support:
 Phone: 421 33 790 2910
Japan Customer Focus Center
 Phone: 81-3-5773-3850

ON Semiconductor Website: www.onsemi.com
Order Literature: http://www.onsemi.com/orderlit
 For additional information, please contact your local Sales Representative